Biochemistry

 Volume 28, Number 19 September 19, 1989

Perspectives in Biochemistry

Long-Range Electron Transfer in Multisite Metalloproteins†

Harry B. Gray* and Bo G. Malmström‡
Arthur Amos Noyes Laboratory, California Institute of Technology, Pasadena, California 91125
Received March 1, 1989; Revised Manuscript Received April 27, 1989

Electron-transfer (ET)[1] reactions play major roles in respiration and photosynthesis. In both of these processes, there are electron-transport chains associated with specific cell organelles. These chains consist of a number of ET complexes firmly bound to biological membranes. ET between the complexes is mediated by small, diffusible molecules. The ET components within the complexes are flavins, iron–sulfur clusters, heme-bound iron, and manganese and copper ions. The complexes span the membranes, and ET through them is coupled to the translocation of protons across the membranes. This leads to the creation of an electrochemical potential, which drives the synthesis of ATP according to the chemiosmotic mechanism of Mitchell (1966).

Biological ET reactions have a number of characteristics distinguishing them from most redox processes involving small metal complexes. First, they occur rapidly over large molecular distances (>10 Å). Second, the ET event is often accompanied by only minor changes in the structure of the redox site. Finally, many biological ET complexes are molecular ion pumps, whose operation requires a structural control of the electron flow.

A good deal is known about the factors governing short-range ET in metal complexes (Taube, 1984; Marcus & Sutin, 1985), whereas the understanding is less complete concerning long-range ET in biological systems. In recent years, there has, however, been real progress in the understanding of ET involving small metalloproteins such as plastocyanin and cytochrome *c* (Sykes, 1985; Scott et al., 1985). In addition, there has been a considerable amount of experimental work with artificial multisite metalloproteins, aimed at illuminating the effects of the driving force, the reorganization energy, the distance, and the intervening medium on the rate of long-range ET. In this paper, we will review the current status of such model studies. To set the scene, this review will be preceded by a short discussion of biological ET, in particular the different properties needed in proteins, like cytochrome *c*, which mediate ET alone compared to proteins in which the ET is coupled to the pumping of protons. In the concluding section of the paper, the lessons learned from the model studies will be applied to one particular proton pump, cytochrome oxidase.

Electron Transfer in Biology

There are great similarities in the types of ET complexes encountered in respiration and photosynthesis, as illustrated in Figure 1. In both cases, ET between complexes is mediated by a quinone at one point and by a small, water-soluble metalloprotein at another. In particular, the composition of complex III in respiration is nearly identical with that of the b_6f complex in photosynthesis. Proton translocation occurs at these complexes and also at complexes I and IV (cytochrome oxidase) in respiration (Wikström & Saraste, 1984).

Mitchell (1966) suggested the redox loop as a device for achieving proton translocation. [The Q-cycle (Mitchell, 1975), believed to operate in the bc_1 (complex III) and b_6f complexes, is a variation of the redox loop concept.] The redox loop is defined as a system that translocates hydrogen atoms one way across the membrane and electrons the other way, leaving the proton on one side of the membrane. Thus, a net translocation of protons is accomplished with a H^+/e^- stoichiometry of 1 only. There is, however, good experimental evidence that, in complexes I and IV of respiration, the stoichiometry is actually 2 H^+/e^- (Wikström & Saraste, 1984; Brown & Brand, 1988). With cytochrome oxidase (complex IV), it has been established that 1 H^+/e^- is pumped across the membrane (Wikström, 1977) and, in addition, that the protons consumed in the reduction of dioxygen to water are specifically taken up from the matrix side of the inner mitochondrial membrane

†Our research on protein electron transfer is supported by grants from the National Science Foundation, the National Institutes of Health (H.B.G.), and the Swedish Natural Science Research Council (B.G.M.). This is Contribution No. 7913 from the Arthur Amos Noyes Laboratory.

‡Visiting Associate of the Beckman Institute, California Institute of Technology. Permanent address: Department of Biochemistry and Biophysics, Chalmers University of Technology, S-41296 Göteborg, Sweden.

[1] Abbreviations: a, ammine; cyt, cytochrome; Mb, sperm whale myoglobin; cyt *c*-Zn, zinc derivative of horse heart cytochrome *c*; Mb-ZnP, zinc mesoporphyrin IX derivative of sperm whale myoglobin; ET, electron transfer; isn, isonicotinamide; P, mesoporphyrin IX; py, pyridine.

0006-2960/89/0428-7499$01.50/0

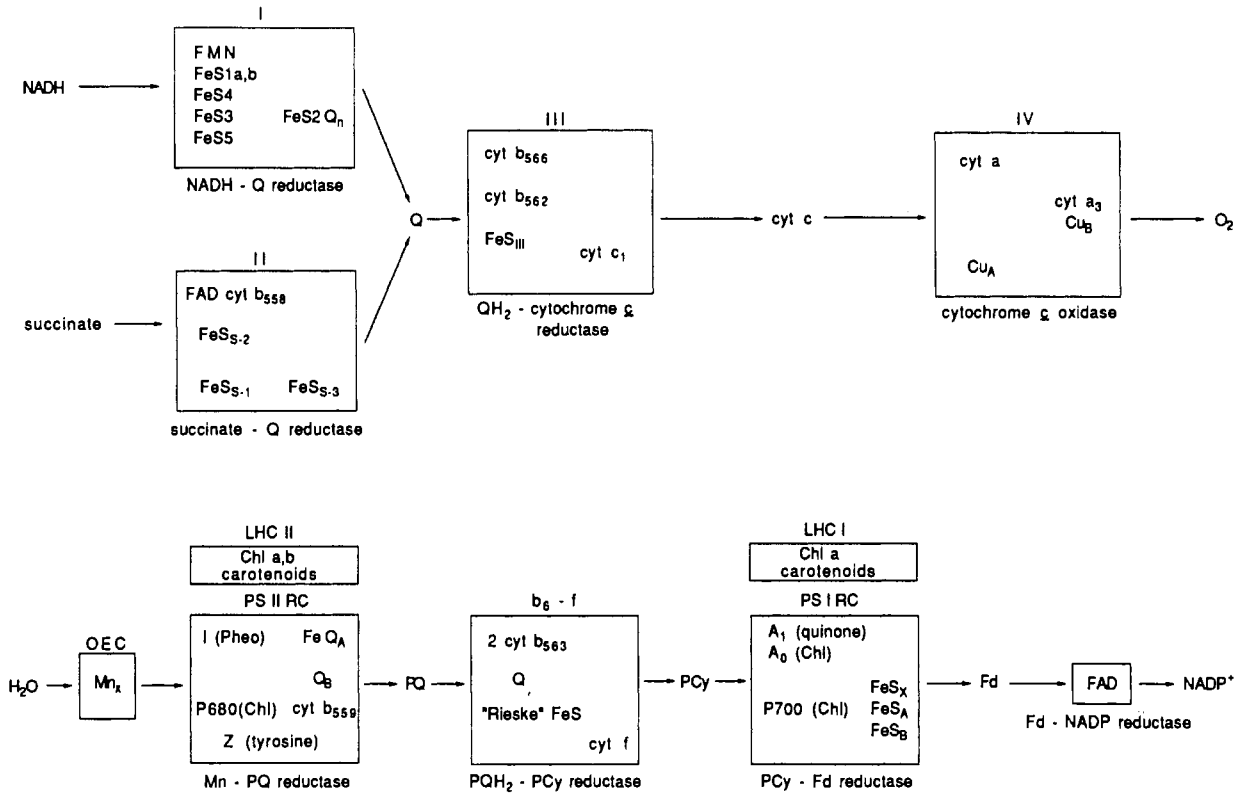

FIGURE 1: ET chains of respiration and photosynthesis. Abbreviations: Q, ubiquinone; PQ, plastoquinone; cyt, cytochrome; FeS, iron–sulfur cluster; PCy, plastocyanin, Fd, ferredoxin; Chl, chlorophyll; Pheo, pheophytin; OEC, oxygen-evolving complex, LHC, light-harvesting complex; PS, photosystem; RC, reaction center.

(Wikström, 1988). In this way, an effective H^+/e^- stoichiometry of 2 is obtained.

Any redox-linked proton pump must follow certain basic principles, as summarized in the cubic reaction scheme of Wikström and Krab (1979). One important feature of this scheme is the existence of separate input and output states for H^+ and e^-. In this way, the ET from donor to acceptor cannot be completed unless the transducer undergoes a transition from the input to the output state. If the e^- input–output states are also the input–output states for H^+, and the transition between states can only occur when the pump is protonated, then the ET reactions will drive proton pumping.

From what has just been said, it is obvious that in redox-linked proton pumps there must be redox-induced conformatonal changes that drastically alter the ET properties of specific redox sites, as will be illustrated later with cytochrome oxidase as an example. Small ET proteins with a single redox site, on the other hand, display minimal structural changes on reduction and reoxidation. Thus, the reorganization energy, which, as will be discussed shortly, is a major determinant of the ET rate, is minimized, and electron transfer is rapid. Good examples are cytochrome *c* and plastocyanin, the proteins that transfer electrons between membrane-bound complexes in respiration and photosynthesis, respectively.

It has been shown (Gray & Malmström, 1983) that the facile ET kinetic properties of blue copper proteins, such as plastocyanin, can be explained in terms of a "rack mechanism" (Lumry & Eyring, 1954; Eyring et al., 1956). According to this hypothesis, functional groups in a protein are in a strained configuration induced by the overall conformation. In plastocyanin, this results in the unusual situation that the metal ligands have almost the same positions in the Cu(II) and the Cu(I) state as well as in the apoprotein (Freeman, 1981). The strained configuration is also evidenced by the high reduction potentials and unusual spectroscopic properties of blue copper proteins (Gray & Malmström, 1983; Ainscough et al., 1987).

Modified Proteins: Intramolecular Electron Transfer at Fixed Distances

Modification of a single-site metalloprotein with a redox-active complex produces a two-site (donor–acceptor) system that allows long-range ET through a protein to be studied in a systematic manner. Ruthenium ammines have been used as modification agents primarily because they can be attached specifically to surface histidines, and the resulting complexes are kinetically stable in solution in the relevant oxidation states (Gray, 1986; Mayo et al., 1986; Osvath et al., 1988). Crystal structure analyses are available for the proteins that have been investigated, and so the distances and intervening media between the donor and acceptor sites in the modified derivatives are known.

Distance Dependence of ET Rates in Heme Proteins. In the analyses that follow, we will assume that the intramolecular ET rate constant is the product of a nuclear frequency factor, ν_n, an electronic factor, Γ, and an activation energy term, $\exp(-\Delta G^*/RT)$ (Lieber et al., 1987):

$$k_{ET} = \nu_n \Gamma \exp(-\Delta G^*/RT) \quad (1)$$

The frequency factor, ν_n, is generally taken to be 10^{13} s^{-1}. The electronic factor, Γ, is unity when the donor and acceptor are strongly coupled, but at long donor–acceptor distances in protein ET reactions the coupling will be much weaker. For such weakly coupled systems, Γ is expected to fall off exponentially with distance (d):

$$\Gamma = \Gamma(d_0) \exp[-\beta(d - d_0)] \quad (2)$$

In eq 2, d_0 is the van der Waals contact distance, usually assumed to be 3 Å (Marcus & Sutin, 1985). The rate of the decrease in electronic coupling with increasing distance is given by β, which depends on the nature of the medium.

Table I: ET Distances and Rates for Ruthenium-Labeled Heme Proteins

derivative	distance (Å)[a]	k_{ET} (s^{-1})[b]
a_5Ru(His-33)cyt *c*-Zn	10.8–11.7 (11.6)	7.7×10^5
a_5Ru(His-48)Mb-ZnP	11.8–16.6 (12.7)	7.2×10^4
a_5Ru(His-81)Mb-ZnP	18.8–19.3 (19.3)	1.5×10^2
a_5Ru(His-116)Mb-ZnP	19.8–20.4 (20.1)	3.0×10^1
a_5Ru(His-12)Mb-ZnP	21.5–22.3 (22.0)	1.4×10^2

[a] The donor–acceptor edge–edge distances are lower and upper values estimated by Lieber et al. (1987). The value for the lowest energy conformation is in parentheses. [b] Rate for Mb-ZnP* → Ru^{III} (Axup et al., 1988; R. K. Upmacis, S. S. Kim, F.-D. Tsay, D. E. Malerba, J. R. Winkler, and H. B. Gray, unpublished results) or cyt *c*-Zn* → Ru^{III} ET (Elias et al., 1988).

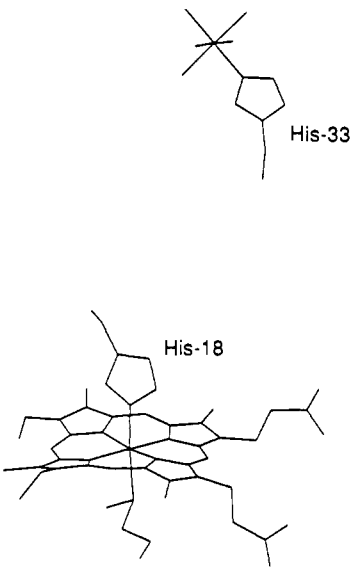

FIGURE 2: View of the ET centers in a_5Ru(His-33)cyt *c*. The distance between the two redox units is 11.6 Å (see Table I).

Sperm whale myoglobin (Mb) has four surface histidines (His-48, His-81, His-116, His-12) that can be modified with ruthenium ammines. Pentaammineruthenium(III) (a_5Ru) has been covalently attached to these histidines. After separation and purification of the reaction products, four singly labeled myoglobin species are obtained (Crutchley et al., 1986; Axup et al., 1988; Karas, 1989). In contrast to the myoglobin system, horse heart cytochrome *c* has only one surface histidine (His-33) that readily binds ruthenium (Yocom et al., 1982). The edge-to-edge distance from the histidine to the heme in each of the a_5RuMb and a_5Rucyt *c* derivatives is given in Table I. The two ET units in a_5Ru(His-33)cyt *c* are shown in Figure 2.

ET rates in photoactive zinc derivatives of a_5RuMb and a_5Ru(His-33)cyt *c* have been measured by transient absorption spectroscopy. In Mb, the heme group can be replaced by zinc mesoporphyrin IX (ZnP) (Axup et al., 1988); in cyt *c*, Zn for Fe substitution gives cyt *c*-Zn (Elias et al., 1988). A laser flash generates triplet ZnP* (or triplet cyt *c*-Zn*), which subsequently returns to the ground state by ET as well as by the usual decay pathways:

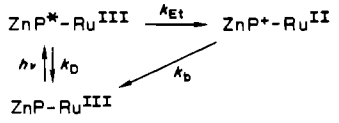

Rates for the a_5RuMb-ZnP and a_5Ru(His-33)cyt *c*-Zn ET reactions are given in Table I. These data are incorporated in two ln k_{ET} versus distance plots shown in Figure 3. A fit

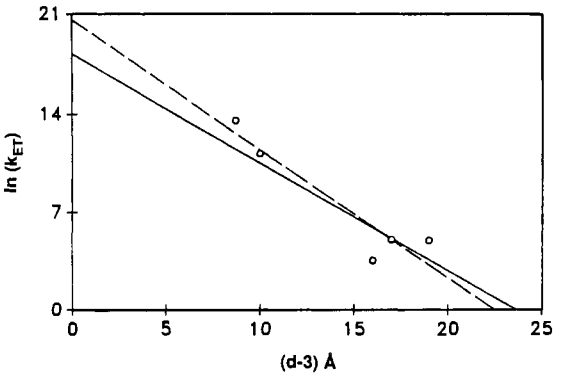

FIGURE 3: ET rate versus distance for Ru-labeled Mb and cyt *c* derivatives. Data are given in Table I. Solid line, $\beta = 0.78$ Å^{-1}; dashed line, $\beta = 0.91$ Å^{-1}.

to all five points gives $\beta = 0.91$ Å^{-1}; restricting the fit to the Mb data yields $\beta = 0.78$ Å^{-1}.

An important conclusion can be drawn immediately from each of the plots: namely, that the edge–edge distance or some through-protein bond pathway related to it is a reasonable indicator of the long-range electronic coupling. An exclusively peptide backbone pathway for Mb ET can be ruled out, because the through-backbone distances are of the order 210, 56, 110, and 380 Å from the proximal histidine to His-48, -81, -116, and -12, respectively, and show no systematic variation with ET rate (Cowan et al., 1989).

In the particular case of a_5Ru(His-12)Mb-ZnP, which displays a slightly higher rate than would be expected from the edge–edge distance, the possibility of a medium effect involving the Trp-14 aromatic group, which lies in a parallel orientation directly along the ET pathway, has been mentioned (Axup et al., 1988). Work on MgP diacid and diester substituted a_5RuMb derivatives also indicates that intervening aromatic residues increase the rate of ET in proteins (Cowan & Gray, 1988; Cowan et al., 1989).

It might be expected that β would be larger for proteins, since direct through-bond pathways are not available. Possibly related to this point is the observation that the maximum rates for intramolecular ET in organic donor–acceptor molecules with rigid spacers are significantly larger than those for Ru-labeled protein systems at similar distances (Mayo et al., 1986; Closs & Miller, 1988). It has been suggested that this difference arises because there are always weakly (noncovalently) coupled units (van der Waals and H-bonded atoms) along the long-range pathway for protein ET reactions (Cowan et al., 1989).

Marcus Theory: Role of the Reorganization Energy

According to Marcus, the activation free energy for ET (ΔG^*, eq 1) depends on the reaction free energy, $\Delta G°$, and the nuclear reorganization energy, λ (Marcus & Sutin, 1985):

$$\Delta G^* = (\Delta G° + \lambda)^2/4\lambda \quad (3)$$

As the reaction free energy is increased, the ET rate is predicted to increase, reach a maximum when $-\Delta G° = \lambda$, and then fall off (Figure 4). The highly exoergic region where the ET rate is predicted to decrease is called the "inverted region".

Both driving force and temperature effects on ET rates have been investigated in attempts to evaluate the reorganization energy accompanying protein ET. Measurements of ET in protein–protein complexes have been analyzed in terms of λ values ranging from 0.8 eV for the cyt *c*/cyt b_5 complex (McLendon, 1988) to 2.1 eV for a Zn,Fe hybrid hemoglobin

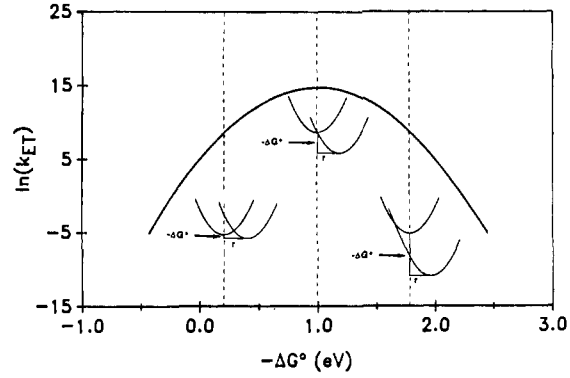

FIGURE 4: Dependence of the ET rate on driving force for a system following eq 3 in which the reorganization energy is 1 eV. Shown under the Marcus curve are reactant–product energy surfaces at driving forces of 0.2, 1.0, and 1.8 eV. The product $\nu_n\Gamma$ is 2.8×10^6 s^{-1} in all three cases.

Table II: ET Rates in Ru(His-33)cyt *c* Derivatives[a]

donor	acceptor	$-\Delta G°$ (eV)	k_{ET} (s^{-1})
a_5Ru^{II}	cyt *c*-Fe^{III}	0.18	3.0×10^1
a_5Ru^{II}	cyt *c*-Zn^*	0.36	2.4×10^2
a_4isnRu^{II}	cyt *c*-Zn^+	0.66	2.0×10^5 (k_b)
cyt *c*-Zn^*	a_5Ru^{III}	0.70	7.7×10^5
a_4pyRu^{II}	cyt *c*-Zn^+	0.74	3.5×10^5 (k_b)
cyt *c*-Zn^*	a_4pyRu^{III}	0.97	3.3×10^6
a_5Ru^{II}	cyt *c*-Zn^+	1.01	1.6×10^6 (k_b)
cyt *c*-Zn^*	a_4isnRu^{III}	1.05	2.9×10^6

[a] From Meade et al. (1989).

(Peterson-Kennedy et al., 1986), and reorganization energies of 0.7 and 1.2 eV have been estimated from the kinetics of the cyt *c* and cyt b_5 ET self-exchange reactions (Dixon et al., 1989). We shall concentrate on two Ru-modified protein systems, a_4LRu(His-33)cyt *c* and a_4LRu(His-48)Mb (L = NH_3, py, isn), because the data available in these cases are quite extensive and the ET distances and intervening media are fixed and known.

Ruthenated Cytochrome c. The ET rates for a_4LRu(His-33)cyt *c*-M (M = Fe, Zn) vary from 3.0×10^1 to 3.3×10^6 s^{-1} over a 0.18–1.05-eV range of driving forces (Table II). The cyt *c*-$Zn^* \rightarrow Ru^{III}$ and $Ru^{II} \rightarrow ZnP^+$ reactions with comparable driving forces proceed at comparable rates in Rucyt *c*-Zn derivatives, thereby indicating that these ET processes have similar values of λ and Γ. It is not likely, however, that the same holds for the Rucyt *c*-Fe ($Ru^{II} \rightarrow Fe^{III}$) ET reaction. If just the Rucyt *c*-Zn reactions are considered, analysis of the rates gives $\lambda = 1.2$ eV and $\nu_n\Gamma = 2.8 \times 10^6$ s^{-1} (Meade et al., 1989). As can be seen from the solid curve in Figure 5, the $Ru^{II} \rightarrow Fe^{III}$ ET reaction proceeds somewhat more slowly than expected, suggesting weaker electronic coupling between the Fe porphyrin and the Ru complex.

Configurational changes of both the inner coordination spheres of the metal centers (λ_i) and the surrounding medium (λ_o) contribute to the total nuclear reorganization energy (λ) in Rucyt *c* ($\lambda = \lambda_i + \lambda_o$). The inner-sphere contribution can be estimated from the structural changes that are known to accompany oxidation of Ru(II) ammines and Zn porphyrins. The Ru–N bond lengths generally change by less than 0.05 Å upon one-electron oxidation of Ru(II) ammine complexes (Gress et al., 1981), and estimates of the inner-sphere reorganization energies are on the order of 0.05 eV (Brown & Sutin, 1979; Siders & Marcus, 1981). An X-ray crystal structure of a Zn porphyrin radical cation reveals fairly small changes in bond lengths and angles compared to the neutral precursor (Collins & Hoard, 1970; Spaulding et al., 1974), and spectroscopic evidence indicates relatively minor distortions of the Zn porphyrin upon excitation to the lowest-lying triplet state (Meade et al., 1989). Hence, the contribution of the inner-sphere configurational changes about the Zn porphyrin is not likely to be more than 0.15 eV, leading to an estimated upper limit of 0.2 eV for the total inner-sphere reorganization barrier in the Rucyt *c* intramolecular ET reactions.

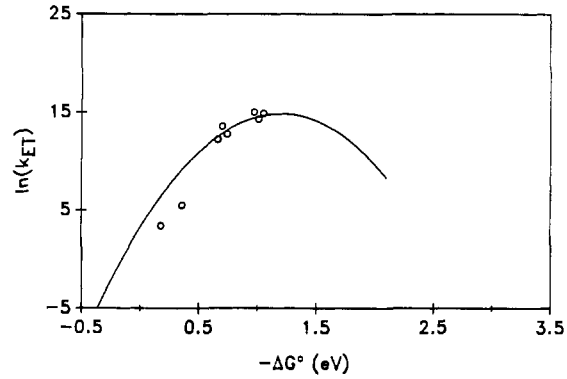

FIGURE 5: ET rate as a function of the free energy change for Rucyt *c* (see Table II). The Marcus curve is for $\lambda = 1.2$ eV.

The remaining contribution to λ in Rucyt *c* must arise from configurational changes of the solvent and polypeptide backbone of the protein (λ_o). Calculations of solvent reorganization energies typically treat the solvent as a dielectric continuum. The original Marcus model, which represents the reactants as two conducting spheres embedded in a dielectric continuum, yields an estimate of 1.1 eV for the solvent reorganization energy in Rucyt *c* (Meade et al., 1989). More sophisticated treatments describe the reorganization energy associated with transferring a single charge from one point to another within spherical or ellipsoidal cavities of low dielectric constant embedded in dielectric continua (Brunschwig et al., 1986). Taking the Rucyt *c* system as a single sphere of 32-Å diameter leads to an estimate of 0.63 eV for the solvent reorganization energy (Meade et al., 1989). Neither solvent model accounts for reorganization of the protein matrix in response to the charge transfer. A calculation of the protein-only reorganization energy accompanying the cyt *c* ET self-exchange reaction indicates a contribution of 0.15 eV from protein dielectric relaxation to λ_o (Churg et al., 1983). The total λ for Rucyt *c* would then be predicted to fall in the 1.0–1.4-eV range, which encompasses the best experimentally derived values.

Ruthenated Myoglobin. The ET rates for a_5Ru(His-48)- and $a_4$pyRu(His-48)-labeled Mb's have been determined with flash photolysis (Karas et al., 1988). The observed ET rate constants are 0.058 s^{-1} for a_5RuMb-Fe and 2.5 s^{-1} for $a_4$pyRuMb-Fe. The Fe^{II}/Ru^{III} ET rate for a_5Ru(His-48)-Mb-Fe is within experimental error of the ET rate previously determined by generating the Ru^{II}/Fe^{III} mixed-valence species. The observation that the rate constant is independent of the initial $[Ru^{III}Fe^{II}]:[Ru^{II}Fe^{III}]$ ratio demonstrates that long-range ET in a_5Ru(His-48)Mb-Fe is reversible. At 25 °C the forward and reverse ET rates are calculated to be 0.04 and 0.02 s^{-1}, respectively.

In order to extend the driving force dependence to large values of $-\Delta G°$ (~1 eV), Mb derivatives were prepared by removing the heme in Ru(His-48)Mb and replacing it with a photoactive porphyrin (MP). Rate constants and driving forces are given in Table III.

The donor orbital of a photoactive porphyrin MP* is more delocalized than the orbital of an iron porphyrin, and therefore, the MP* to Ru electronic coupling should be larger than that

Table III: ET Rates in Ru(His-48)Mb Derivatives[a]

donor	acceptor	$-\Delta G°$ (eV)	k_{ET} (s^{-1})
$Fe^{II}P$	a_5Ru^{III}	0.02	0.040
$Fe^{II}P$	a_4pyRu^{III}	0.28	2.5
H_2P^*	a_5Ru^{III}	0.53	7.6×10^2
PdP*	a_5Ru^{III}	0.70	9.1×10^3
PtP*	a_5Ru^{III}	0.73	1.2×10^4
CdP*	a_5Ru^{III}	0.85	6.3×10^4
MgP*	a_5Ru^{III}	0.87	5.7×10^4
ZnP*	a_5Ru^{III}	0.88	7.0×10^4
PdP*	a_4pyRu^{III}	0.96	9.0×10^4

[a] From Karas et al. (1988) and Cowan et al. (1989).

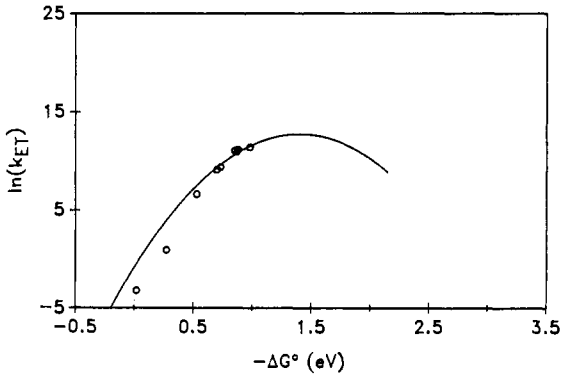

FIGURE 6: Plot of ln k_{ET} versus $-\Delta G°$ for the RuMb ET reactions (see Table III). The Marcus curve is for $\lambda = 1.4$ eV.

between FeP and Ru (Cowan et al., 1989). The best fit to the data for the $MP^* \rightarrow Ru^{III}$ ET reactions yields $\lambda = 1.4$ eV and $\nu_n\Gamma = 3.5 \times 10^5\ s^{-1}$ (Figure 6). The $Fe^{II} \rightarrow Ru^{III}$ rates fall well below the $\lambda \sim 1.4$ eV curve, consistent with the argument that the FeP to Ru electronic coupling is weaker. Another factor in the low $Fe^{II} \rightarrow Ru^{III}$ rates could well be a larger λ associated with the binding of water to the Fe^{III} proteins. Inclusion of the FeP points in the Marcus plot indicates a very high λ ($\sim$2 eV), and the strong temperature dependence of the $Fe^{II} \rightarrow Ru^{III}$ ET rate in a_5Ru(His-48)Mb also is consistent with a relatively large λ (Karas et al., 1988; Cowan & Gray, 1988; Crutchley et al., 1986).

Reorganization Energy Control of Long-Range Protein ET. Work on Ru-modified cytochrome *c* and myoglobin derivatives has shown that long-range ET reactions can be controlled through tradeoffs between driving force and reorganization energy. Since rearrangements of water molecules are usually associated with large reorganization energies, the exclusion of water in either the inner or outer sphere of a donor or acceptor would be expected to lead to much higher ET rates if other factors—notably the driving force—were not changed very much. Alternatively, λ could be reduced by tightening the polypeptide pockets in which the donor and acceptor reside. Reductions in λ by 1 eV or more conceivably could be achieved by a combination of lowering the polarity of the ET medium and tightening its hold on the donor and acceptor, thereby drastically limiting nuclear rearrangements accompanying the reaction. Calculations based on the parameters derived from work on ruthenated proteins show that a protein ET reaction at 0.1-V driving force would increase in rate from 5×10^{-2} to $2 \times 10^4\ s^{-1}$ if λ were reduced from 1.5 to 0.5 eV at a donor–acceptor edge–edge distance of 15 Å (Figure 7).

Cytochrome Oxidase

Cytochrome oxidase contains four redox-active metal centers. Two of them, cytochrome *a* and a_3, contain a heme A group in separate environments, whereas the other two, Cu_A and Cu_B, are copper ions coordinated in different ways to the

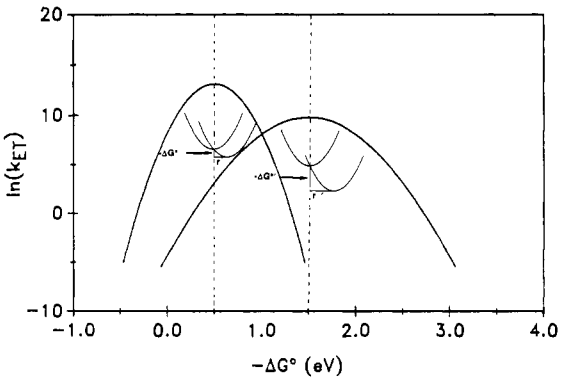

FIGURE 7: Marcus curves showing the dependence of the ET rate on $-\Delta G°$ for λ values of 1.5 and 0.5 eV. These two λ values could be associated with two different enzyme conformations, E_1 ($\lambda = 1.5$ eV) and E_2 ($\lambda = 0.5$ eV). Below the curves are reactant–product energy surfaces for activationless ET ($-\Delta G° = \lambda$). The two curves were calculated for ET at $d = 15$ Å, using parameters derived from work on ruthenated proteins (M. Therien and H. B. Gray, unpublished results).

protein (Wikström et al., 1981). All centers are more than 15 Å from each other, except cytochrome a_3 and Cu_B, which form a binuclear unit. Electrons from cytochrome *c* first reduce Cu_A and cytochrome *a*, which are in rapid redox equilibrium (Antalis & Palmer, 1982). From these reduced centers, they are transferred intramolecularly to the cytochrome a_3–Cu_B center, which is the dioxygen-binding and -reducing site.

The intramolecular ETs from cytochrome *a* and Cu_A to the binuclear site have been thought to limit k_{cat}, the catalytic constant (Wilson et al., 1981; Brzezinski et al., 1986). Both transfers are, however, rapid compared to k_{cat} in the mixed-valence state (Boelens et al., 1982; Brzezinski & Malmström, 1987). Cytochrome *a* and Cu_A are also rapidly oxidized when the fully reduced enzyme is mixed with dioxygen (Hill et al., 1986; Orii, 1988). This suggests that the enzyme can exist in two states, in which the ET properties are different. Since this is a requirement of a proton pump (Blair et al., 1986), it is attractive to consider that these two forms represent the separate input and output states for electrons in the pump redox sites.

There are strong redox interactions between the metal centers (Wikström et al., 1981; Blair et al., 1986). This may also reflect the existence of two conformational states with different ET properties, as the interactions can hardly be electrostatic in origin in view of the large metal–metal distances [cf. Nocera et al. (1984)]. In addition, conformational changes induced by reduction of Cu_A and/or cytochrome *a* have been detected by fluorescence measurements (Copeland et al., 1987) and by drastic changes in the rate of cyanide binding to oxidized cytochrome a_3 (Jones et al., 1984). It has recently been demonstrated that the rate of the conformational change detected by cyanide binding varies with pH in the same way as k_{cat} (Thörnström et al., 1988). This suggests that it is this conformational transition rather than the internal ET which is the rate-limiting step. It also indicates that this transition corresponds to the switch between the input and output states, because it has already been pointed out that the internal ET appears slow only when starting from the fully oxidized enzyme. Finally, it should be mentioned that in the output state the rate of ET between Cu_A and the binuclear unit is almost independent of temperature, the enthalpy of activation being as low as 2.1 kJ·mol^{-1} (Brzezinski & Malmström, 1987).

Gating by Changes in Reorganization Energy. The experimental results summarized earlier on the effects of dis-

tance, driving force, and reorganization energy on the rates of ET in model systems strongly suggest that the most efficient way to gate the electron flow in a redox-linked proton pump is by variations in reorganization energy. The same decrease in rate as is given by an increase in the distance of 10 Å is achieved at relatively low driving forces ($\leq$0.5 eV) by an increase in the reorganization energy of 1 eV (96 kJ·mol^{-1}) (Lieber et al., 1987). Driving force variations by themselves would not change the rate substantially, because it is known that the difference in driving force between the input and output states in cytochrome oxidase is less than 0.2 V (Brzezinski & Malmström, 1987).

The argument just given, together with an analysis of the temperature dependence of the ET from Cu_A to the binuclear site in the mixed-valence cytochrome oxidase (Brzezinski & Malmström, 1987), can be used to formulate a mechanism of electron gating. The enzyme has two conformations, E_1 and E_2, corresponding to the input and output states for e^- and H^+. In E_1, there is a large barrier to ET from Cu_A to the binuclear site. This barrier is assumed to be associated mainly with the electron acceptor, cytochrome a_3–Cu_B, because Cu_A has the same structure in the fully oxidized enzyme as in the mixed-valence state, in which electron equilibration with the binuclear site is rapid, as evidenced by EPR (Clore et al., 1980). Reduction of Cu_A and cytochrome *a*, followed by protonation of the proton-translocating group, leads to a transition from E_1 to E_2. The structure of the oxidized cytochrome a_3–Cu_B site is changed in E_2, as evidenced by the large change in the rate of cyanide binding, in such a way that the reorganization energy is lowered. This could be accomplished by a structural change leading to the dissociation of ligated water molecules, or a change in the coordination geometries of the metal ions themselves, or a combination of both. In any case, the structural change should be such that the oxidized binuclear site in E_2 adopts a structure very close to that of the reduced form, thereby minimizing the reorganization energy. This change would be a type of rack mechanism, first suggested to operate in mitochondrial "energy conservation" by Lumry (1963). To gate the electron flow effectively, λ in E_1 should probably be 1 eV higher than in E_2, as depicted in Figure 7. This is a reasonable rack energy in a multisite metalloprotein [cf. Gray and Malmström (1983)].

Acknowledgments

We thank David Smith and Mike Therien for assistance in preparing the figures and for several helpful discussions.

Registry No. Cytochrome oxidase, 9001-16-5.

References

Ainscough, E. W., Bingham, A. G., Brodie, A. M., Ellis, W. R., Gray, H. B., Loehr, T. M., Plowman, J. E., Norris, G. E., & Baker, E. N. (1987) *Biochemistry 26*, 71–82.

Antalis, T. M., & Palmer, G. (1982) *J. Biol. Chem. 257*, 6194–6206.

Axup, A. W., Albin, M., Mayo, S. L., Crutchley, R. J., & Gray, H. B. (1988) *J. Am. Chem. Soc. 110*, 435–439.

Blair, D. F., Gelles, J., & Chan, S. I. (1986) *Biophys. J. 50*, 713–733.

Boelens, R., Wever, R., & Van Gelder, B. F. (1982) *Biochim. Biophys. Acta 682*, 264–272.

Brown, G. C., & Brand, M. D. (1988) *Biochem. J. 252*, 473–479.

Brown, G. M., & Sutin, N. (1979) *J. Am. Chem. Soc. 101*, 883–892.

Brunschwig, B. S., Ehrenson, S., & Sutin, N. (1986) *J. Phys. Chem. 90*, 3657–3668.

Brzezinski, P., & Malmström, B. G. (1987) *Biochim. Biophys. Acta 894*, 29–38.

Brzezinski, P., Thörnström, P.-E., & Malmström, B. G. (1986) *FEBS Lett. 194*, 1–5.

Churg, A. K., Weiss, R. M., Warshel, A., & Takano, T. (1983) *J. Phys. Chem. 87*, 1683–1694.

Clore, M. G., Andréasson, L.-E., Karlsson, B., Aasa, R., & Malmström, B. G. (1980) *Biochem. J. 185*, 155–167.

Closs, G. L., & Miller, J. R. (1988) *Science 240*, 440–447.

Collins, D. M., & Hoard, J. L. (1970) *J. Am. Chem. Soc. 92*, 3761–3771.

Copeland, R. A., Smith, P. A., & Chan, S. I. (1987) *Biochemistry 26*, 7311–7316.

Cowan, J. A., & Gray, H. B. (1988) *Chem. Scr. 28A*, 21–26.

Cowan, J. A., Upmacis, R. K., Beratan, D. N., Onuchic, J. N., & Gray, H. B. (1988) *Ann. N.Y. Acad. Sci. 550*, 68–84.

Crutchley, R. J., Ellis, Jr., W. R., & Gray, H. B. (1986) *J. Am. Chem. Soc. 107*, 5002–5004.

Dixon, D. W., Xiaole, H., Woehler, S. E., Mauk, A. G., & Sishta, B. P. (1989) *J. Am. Chem. Soc.* (in press).

Elias, H., Chou, M. H., & Winkler, J. R. (1988) *J. Am. Chem. Soc. 110*, 429–434.

Eyring, H., Lumry, R., & Spikes, J. D. (1954) in *The Mechanism of Enzyme Action* (McElroy, W. D., & Glass, B., Eds.) pp 123–136, The John Hopkins Press, Baltimore, MD.

Freeman, H. C. (1981) in *Coordination Chemistry-21* (Laurent, J. P., Ed.) pp 29–51, Pergamon Press, Oxford.

Gray, H. B. (1986) *Chem. Soc. Rev. 15*, 17–30.

Gray, H. B., & Malmström, B. G. (1983) *Comments Inorg. Chem. 2*, 203–209.

Gress, M. E., Creutz, C., & Quicksall, C. O. (1981) *Inorg. Chem. 20*, 1522–1528.

Hill, B. C., Greenwood, C., & Nicholls, P. (1986) *Biochim. Biophys. Acta 853*, 91–113.

Jones, M. G., Bickar, D., Wilson, M. T., Brunori, M., Colosimo, A., & Sarti, P. (1984) *Biochem. J. 220*, 57–66.

Karas, J. L. (1989) Ph.D. Thesis, California Institute of Technology, Pasadena, CA.

Karas, J. L., Lieber, C. M., & Gray, H. B. (1988) *J. Am. Chem. Soc. 110*, 599–600.

Lieber, C. M., Karas, J. L., Mayo, S. L., Albin, M., & Gray, H. B. (1987) *Proceedings of the Robert A. Welch Conference on Chemical Research. Design of Enzymes and Enzyme Models*, Nov 2–4, 1987, pp 9–33, Robert A. Welch Foundation, Houston, TX.

Lumry, R. (1963) in *Photosynthesis Mechanisms of Green Plants*, pp 625–634, Publication No. 1145, National Academy of Sciences, Washington, DC.

Lumry, R., & Eyring, H. (1954) *J. Phys. Chem. 58*, 110–120.

Marcus, R. A., & Sutin, N. (1985) *Biochim. Biophys. Acta 811*, 265–322.

Mayo, S. L., Ellis, W. R., Jr., Crutchley, R. J., & Gray, H. B. (1986) *Science 233*, 948–952.

McLendon, G. (1988) *Acc. Chem. Res. 21*, 160–167.

Meade, T. J., Gray, H. B., & Winkler, J. R. (1989) *J. Am. Chem. Soc. 111*, 4353–4356.

Mitchell, P. (1966) *Chemiosmotic Coupling in Oxidative and Photosynthetic Phosphorylation*, Glynn Research, Bodmin, England.

Mitchell, P. (1975) *FEBS Lett. 59*, 137–139.

Nocera, D. G., Winkler, J. R., Yocom, K. M., Bordignon, E., & Gray, H. B. (1984) *J. Am. Chem. Soc. 106*, 5145–5150.

Orii, Y. (1988) *Chem. Scr. 28A*, 63–69.

Osvath, P., Salmon, G. A., & Sykes, A. G. (1988) *J. Am. Chem. Soc. 110*, 7114–7118.
Peterson-Kennedy, S. E., McGourty, J. L., Kalweit, J. A., & Hoffman, B. M. (1986) *J. Am. Chem. Soc. 108*, 1739–1746.
Scott, R. A., Mauk, A. G., & Gray, H. B. (1985) *J. Chem. Ed. 62*, 932–938.
Siders, P., & Marcus, R. A. (1981) *J. Am. Chem. Soc. 103*, 741–747.
Spaulding, L. D., Eller, P. G., Bertrand, J. A., & Felton, R. H. (1974) *J. Am. Chem. Soc. 96*, 982–987.
Sykes, A. G. (1985) *Chem. Soc. Rev. 14*, 283–315.
Taube, H. (1984) *Angew. Chem., Int. Ed. Engl. 23*, 329–339.
Thörnström, P.-E., Nilsson, T., & Malmström, B. G. (1988) *Biochim. Biophys. Acta 935*, 103–108.
Wikström, M. (1977) *Nature 266*, 271–273.
Wikström, M. (1988) *FEBS Lett. 231*, 247–252.
Wikström, M., & Krab, K. (1979) *Biochim. Biophys. Acta 549*, 177–222.
Wikström, M., & Saraste, M. (1984) in *Bioenergetics* (Ernster, L., Ed.) pp 49–94, Elsevier, Amsterdam.
Wikström, M., Krab, K., & Saraste, M. (1981) *Cytochrome Oxidase—A Synthesis*, Academic Press, London.
Wilson, M. T., Peterson, J., Antonini, E., Brunori, J., Colosimo, A., & Wyman, J. (1981) *Proc. Natl. Acad. Sci. U.S.A. 78*, 7115–7118.
Yocom, K. M., Shelton, J. B., Shelton, J. R., Schroeder, W. A., Worosila, G., Isied, S. S., Bordignon, E., & Gray, H. B. (1982) *Proc. Natl. Acad. Sci. U.S.A. 79*, 7052–7055.

Accelerated Publications

Escherichia coli Initiation Factor 3 Protein Binding to 30S Ribosomal Subunits Alters the Accessibility of Nucleotides within the Conserved Central Region of 16S rRNA†

Parimi Muralikrishna‡,§ and Eric Wickstrom*,‖

Departments of Chemistry, Biochemistry and Molecular Biology, and Surgery, University of South Florida, Tampa, Florida 33620

Received July 5, 1989; Revised Manuscript Received July 26, 1989

ABSTRACT: Translational initiation factor 3 (IF3) is an RNA helix destabilizing protein which interacts with strongly conserved sequences in 16S rRNA, one at the 3′ terminus and one in the central domain. It was therefore of interest to identify particular residues whose exposure changes upon IF3 binding. Chemical and enzymatic probing of central domain nucleotides of 16S rRNA in 30S ribosomal subunits was carried out in the presence and absence of IF3. Bases were probed with dimethyl sulfate (DMS), at A(N-1), C(N-3), and G(N-7), and with *N*-cyclohexyl-*N*′-[2-(*N*-methyl-4-morpholinio)ethyl]carbodiimide *p*-toluenesulfonate (CMCT), at G(N-1) and U(N-3). RNase T1 and nuclease S1 were used to probe unpaired nucleotides, and RNase V1 was used to monitor base-paired or stacked nucleotides. 30S subunits in physiological buffers were probed in the presence and absence of IF3. The sites of cleavage and modification were detected by primer extension. IF3 binding to 30S subunits was found to reduce the chemical reactivity and enzymatic accessibility of some sites and to enhance attack at other sites in the conserved central domain of 16S rRNA, residues 690–850. IF3 decreased CMCT attack at U701 and U793 and V1 attack at G722, G737, and C764; IF3 enhanced DMS attack at A814 and V1 attack at U697, G833, G847, and G849. Many of these central domain sites are strongly conserved and with the conserved 3′-terminal site define a binding domain for IF3 which correlates with a predicted cleft in two independent models of the 30S ribosomal subunit.

Escherichia coli IF3[1] is a basic polypeptide of 180 residues, 20 520 g/mol (Sacerdot et al., 1982), which catalyzes efficient translation of mRNA bound to 30S ribosomal subunits (Gualerzi et al., 1986; Calogero et al., 1988). Under physiological ionic conditions, IF3 binds to free 30S ribosomal subunits, inhibiting their association with 50S ribosomal subunits to form 70S ribosomes (Goss et al., 1982), unless both mRNA and fMet-tRNA have bound to form an initiation complex.

Extensive studies of the structure of 30S ribosomal subunits, 16S rRNA, and the 30S ribosomal proteins have led to consensus models for the secondary structure of 16S rRNA and the sites of RNA–protein interactions within the subunit (Brimacombe, 1988; Stern et al., 1989). However, the functional roles of most parts of the 30S subunit remain unknown. In particular, the structural transitions which IF3

† This work was supported by NIH Grant GM32024 to E.W.
* Address correspondence to this author at the Department of Chemistry.
‡ Department of Chemistry.
§ Present address: Department of Chemistry, University of Pennsylvania, Philadelphia, PA 19104.
‖ Departments of Chemistry, Biochemistry and Molecular Biology, and Surgery.

[1] Abbreviations: CMCT, *N*-cyclohexyl-*N*′-[2-(*N*-methyl-4-morpholinio)ethyl]carbodiimide *p*-toluenesulfonate; DMS, dimethyl sulfate; DTT, dithiothreitol; EDTA, (ethylenedinitrilo)tetraacetate; IF, initiation factor; RNase, ribonuclease; $NaDodSO_4$, sodium dodecyl sulfate.

0006-2960/89/0428-7505$01.50/0